

# Supporting Information

for

## Growth Modes and Quantum Confinement in Ultrathin Vapour-Deposited MAPbI<sub>3</sub> Films

*Elizabeth S. Parrott, Jay B. Patel, Amir-Abbas Haghighirad<sup>+</sup>, Henry J. Snaith, Michael B. Johnston,*

*Laura M. Herz\**

Department of Physics, University of Oxford, Clarendon Laboratory, Parks Road, Oxford OX1 3PU,

UK

+ Karlsruhe Institute of Technology, 76021 Karlsruhe, Germany

\*[laura.herz@physics.ox.ac.uk](mailto:laura.herz@physics.ox.ac.uk)

## Optical Thickness Determination

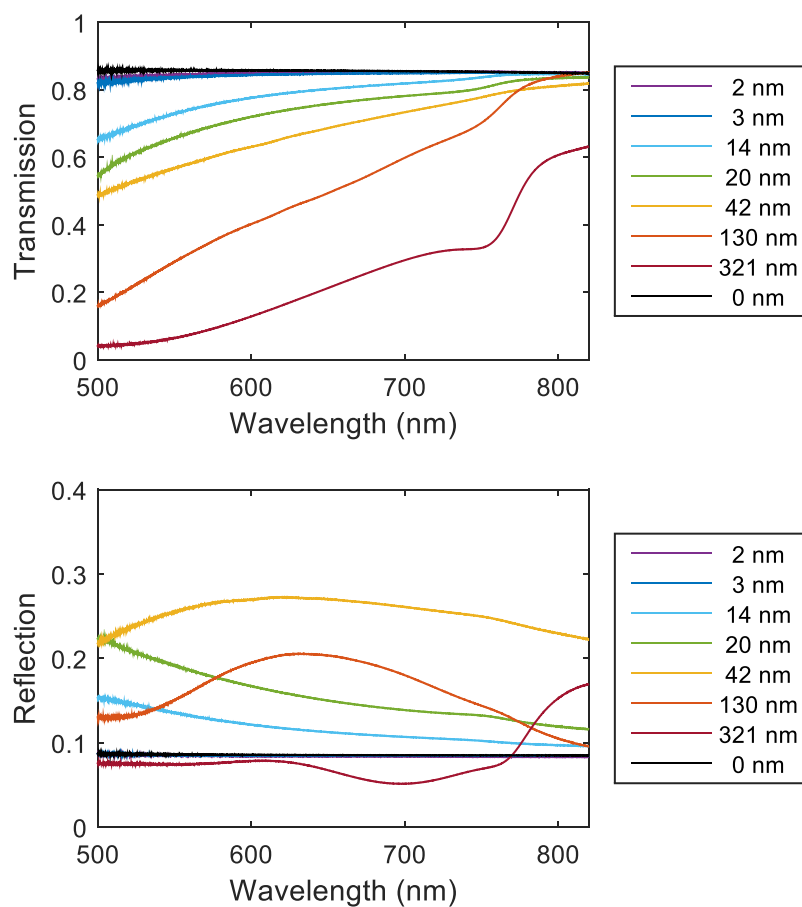


**Figure S1:** Proportion of light transmitted (a) or reflected (b) through MAPbI<sub>3</sub> thin film on quartz samples of various optical thickness made by increasing vapour deposition time. 0 nm indicates the blank quartz substrate.

We determined the absorbance by measuring the reflection and transmission of the thin films.

From Beer's law, the absorbance is

$$a = \log((1-R)/T) \quad (\text{Equation S1})$$

and also

$$a = \alpha D + b \quad (\text{Equation S2})$$

where  $b$  is the measurement background,  $D$  is the film thickness and  $\alpha$  is the absorption coefficient.

In order to find the optical thickness,  $D$ , we matched the absorbance,  $a$ , for each sample to a known absorption coefficient,  $\alpha$ . We used values of  $\alpha$  for similarly prepared MAPbI<sub>3</sub> films, determined by Crothers et al.<sup>3</sup>, and in good agreement with Davies et al.<sup>4</sup>

To improve accuracy we matched our calculated absorbance to the absorption coefficient across the range 550-700 nm, instead of matching at only a single wavelength point. To achieve this we plotted  $\alpha$  against  $a$ , and fitted the linear equation  $\alpha = (a-b)/D$ , such that the gradient of the fit gave us  $1/D$ . The value of  $b$  was constrained to keep the below-band-gap absorption close to zero.

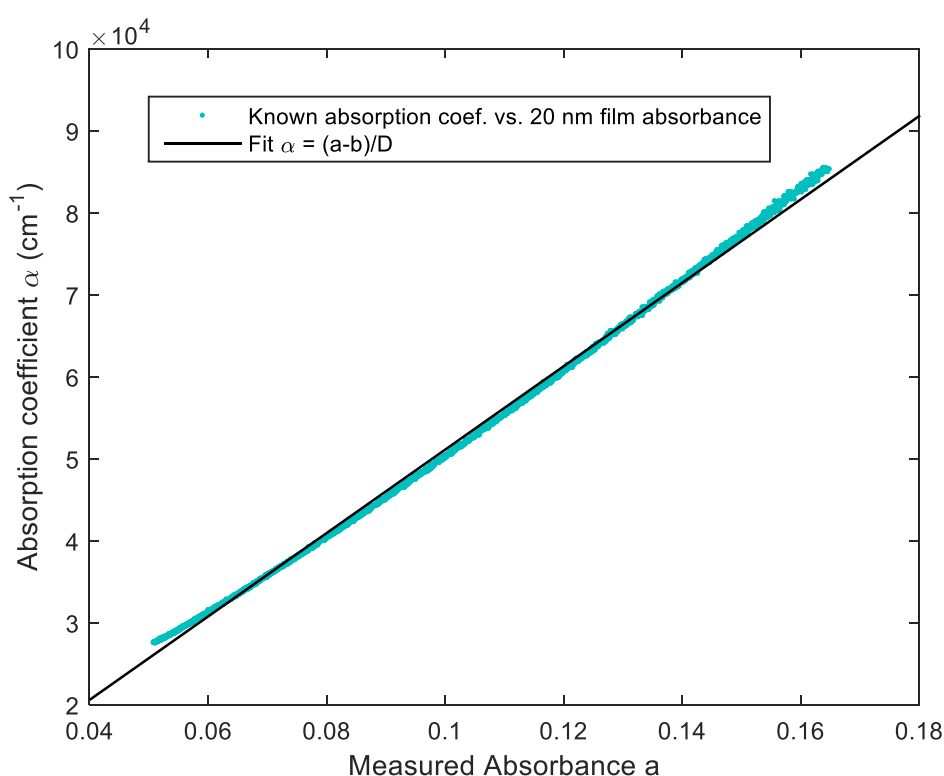


**Figure S2:** Example of fit to determine optical thickness  $D$  by plotting a known absorption coefficient (taken from Reference 3) against the absorption (from 550-700 nm) of a MAPbI<sub>3</sub> thin film sample from the batch with 240s deposition time, giving  $D = 20$  nm.

The absorption coefficient calculated from the fitting parameters for each sample ( $\alpha = (a-b)/D$ ) is shown in Figure S3, showing there is an acceptable match.

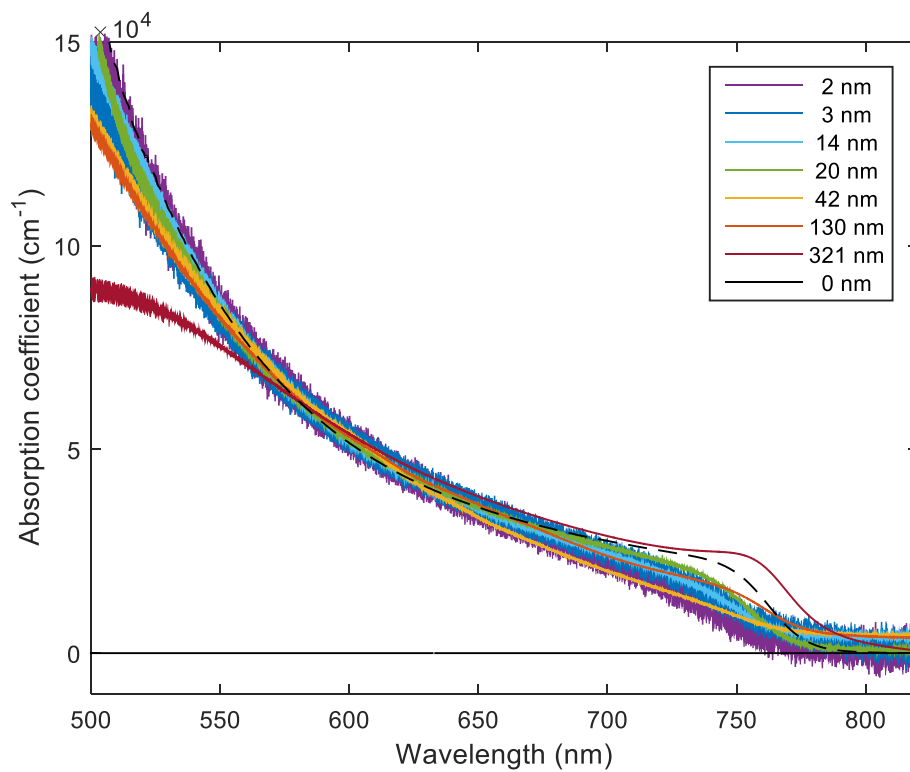


**Figure S3:** Absorption coefficient for each MAPbI<sub>3</sub> thin film sample calculated from measured absorbance using the optical thickness given in the legend. The black dashed line is the average absorption coefficient determined by Crothers et al.<sup>3</sup>

## XRD Analysis

The X-ray diffraction spectra are shown in Figure S4. The spectra were fitted with a Pseudo-Voigt function using the general structural analysis software (GSAS) to extract the peak position and the full width half maximum (FWHM).

The angle of the peaks was corrected for sample tilt by using the quartz peak at  $16.433^\circ$  as a reference.

The d-spacing for each thickness was found from the angle of the perovskite (100) and (200) peaks using Bragg's law:

$$2d \sin \theta = n\lambda \quad (\text{Equation S3})$$

where  $n = \sqrt{h^2 + k^2 + l^2}$  for (hkl) is equal to 1 for (100) and 2 for (200).

We take the unstrained d-spacing to be  $d_0 = 6.275 \text{ \AA}$ , the value measured for our thickest sample, since this value falls within the range of previously measured values for unstrained MAPbI<sub>3</sub>.<sup>5-7</sup> The relative strain,  $\epsilon$ , normal to the (100) direction is found using the equation

$$\epsilon = \frac{d_s - d_0}{d_0} \quad (\text{Equation S4})$$

where  $d_s$  is the d-spacing of the sample. The results are shown in Table S1.

Optical thickness/nm	2	3	14	20	42	130	320
Angle of (100)/deg.	14.0213	14.0011	14.0417	14.0534	14.1017	14.0950	14.1018
d-spacing of (100)/ $\text{\AA}$	6.2956	6.3202	6.3020	6.2968	6.2789	6.2780	6.2752
d-spacing of (200)/ $\text{\AA}$	6.2852	6.3157	6.3107	6.3023	6.2880	6.2786	6.2748
<b>Mean d-spacing/<math>\text{\AA}</math></b>	<b>6.2905</b>	<b>6.318</b>	<b>6.3065</b>	<b>6.2995</b>	<b>6.2835</b>	<b>6.2784</b>	<b>6.275</b>
Error: d(100)-d(200)	0.0104	0.0044	0.0087	0.0055	0.0091	0.0006	0.0004
<b>Strain (%)</b>	<b>0.247</b>	<b>0.685</b>	<b>0.502</b>	<b>0.390</b>	<b>0.135</b>	<b>0.054</b>	<b>0.000</b>

**Table S1:** Calculated pseudo-cubic lattice parameters for the two perovskite peaks (100) and (200) in the XRD spectra for each of the MAPbI<sub>3</sub> thin-film samples, and strain calculated from the mean lattice parameter.

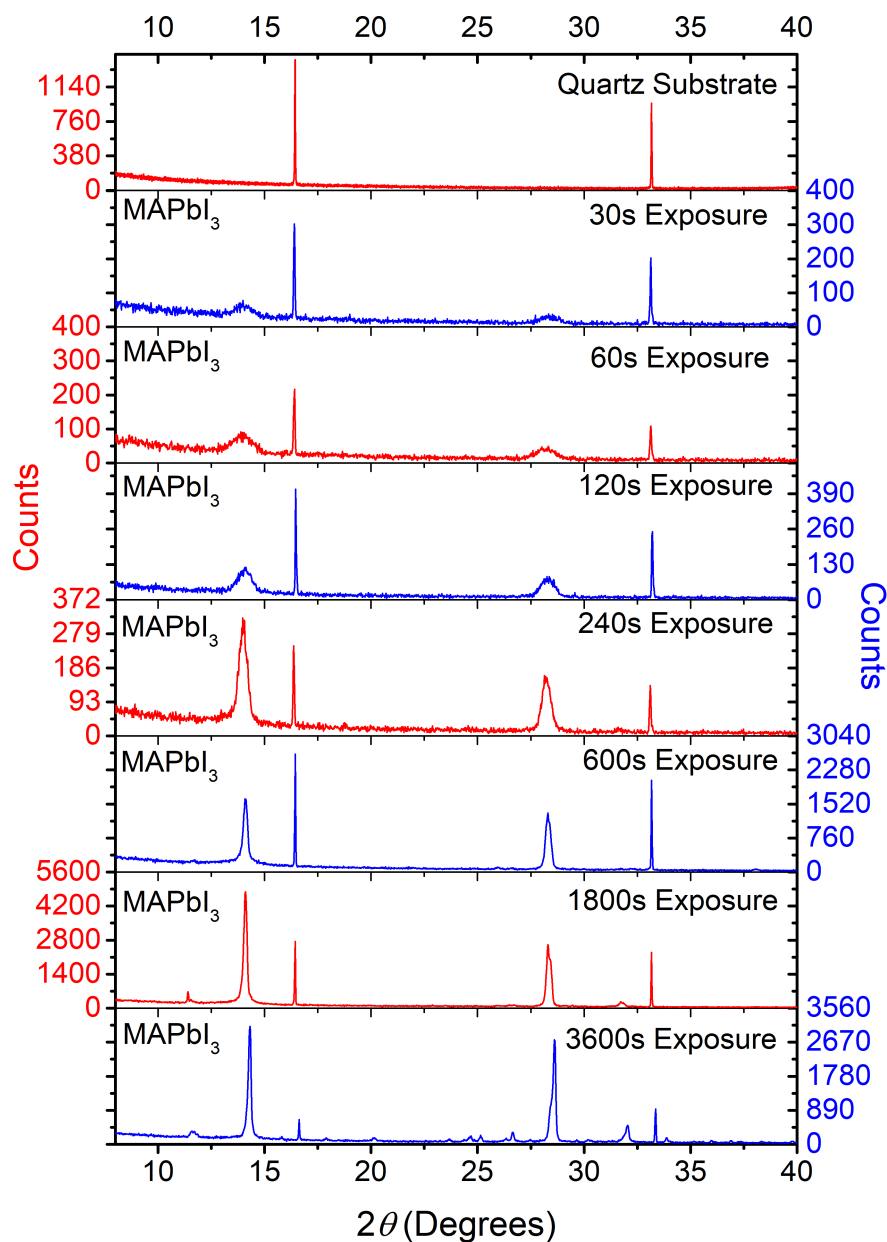


**Figure S4:** X-ray diffraction spectra of MAPbI<sub>3</sub> thin films obtained at a scan speed of 0.4 °/s for 30 minutes using a Cu-K $\alpha$  radiation source at  $\lambda = 1.54 \text{ \AA}$  operating at 40 kV and 40 mA. Vapour exposure times from 300-3600 s in the evaporator correspond to perovskite optical thicknesses of 2-320 nm.

## Scherrer Equation

Smaller grains lead to larger FWHM since there are fewer aligned crystal planes to contribute to diffraction. The grain size can therefore be found from the full width at half maximum (FWHM) of the perovskite peaks, using the Scherrer equation,<sup>8</sup>

$$D = \frac{K \lambda}{\beta \cos \theta} \quad (\text{Equation S5})$$

where  $D$  is the crystallite size,  $\beta$  is the FWHM in radians,  $\lambda = 0.15406$  nm is the wavelength of the X-rays,  $\theta$  is the Bragg angle, and  $K$  is known as the shape factor which is determined by the definition of the peak breadth and the shape of the crystallite. Using the FWHM as the measure of peak breadth,  $K = 0.8859$  gives the height of the crystallite perpendicular to the substrate.<sup>9</sup>

The resolution of the XRD spectrometer leads to angle-dependent instrument broadening, which must be corrected for. We measured the XRD spectrum of a silicon reference and determined the FWHM of each of the peaks. We plot the FWHM against angle in Figure S5, and fit a polynomial. From this fit, we can find the instrument broadening at the relevant angle:  $\beta_{\text{inst}} = 0.062^\circ$  at  $2\theta = 14^\circ$ . We then found the corrected FWHM for each MAPbI<sub>3</sub> sample using the equation

$$\beta^2 = \beta_{\text{sample}}^2 - \beta_{\text{inst}}^2 \quad (\text{Equation S6})$$

The corrected FWHM and the values of crystallite size calculated from Equation S5 are found in Table S2. The FWHM is only accurate to two decimal places, but all decimal places were used in calculations before rounding the final result.

<b>Optical thickness/nm</b>	<b>2</b>	<b>3</b>	<b>14</b>	<b>20</b>	<b>42</b>	<b>130</b>	<b>320</b>
FWHM (100) /degrees	0.9266	1.0889	0.7429	0.4597	0.2216	0.1695	0.1602
Corrected FWHM (100) /degrees	0.9245	1.0871	0.7403	0.4555	0.2127	0.1578	0.1477
<b>Crystallite size/nm</b>	<b>8.7</b>	<b>7.4</b>	<b>10.9</b>	<b>17.7</b>	<b>37.9</b>	<b>51.1</b>	<b>54.6</b>

**Table S2:** Full width at half maximum measured for the (100) peak for each of the samples, full width at half maximum for the same peak corrected for instrument broadening using Equation S6, and the crystallite size determined from equation S5 using  $\lambda = 0.15406$  nm,  $K = 0.8859$ ,  $\beta$  from the corrected FWHM in this table, and  $\theta$  from Table S1.

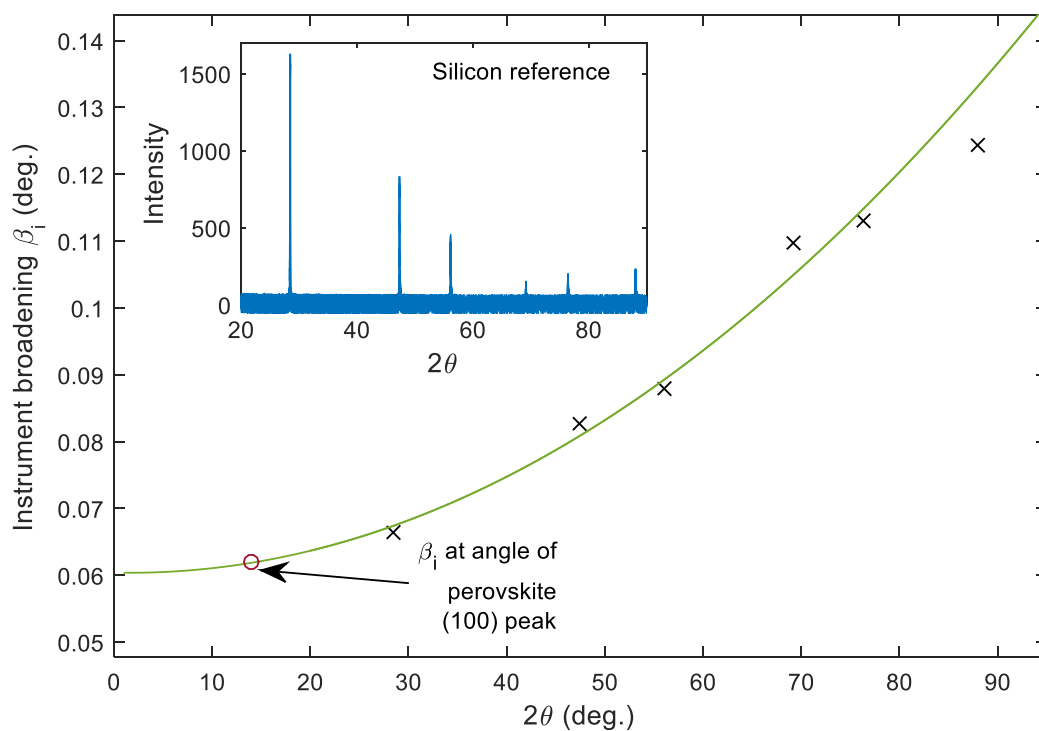


**Figure S5:** Width of the XRD diffraction peak at half maximum for each reflection from the silicon reference as a function of angle (crosses), fitted with a quadratic (green line) which gives instrument broadening as a function of angle. The instrument broadening at  $14^\circ$ , which we use to correct the FWHM of the perovskite (100) peak, is marked with a red circle. Inset: XRD spectrum of the silicon reference sample used to calculate instrument broadening.

## Williamson-Hall Plot

The Scherrer formula is only valid when the crystallite size is the main contribution and broadening due to micro-strain (i.e. the distribution of lattice plane spacing in the sample) can be neglected. When microstrain is included, the formula is given by

$$\beta = \frac{K \lambda}{D \cos \theta} + 4\epsilon \tan \theta \quad (\text{Equation S7})$$

This expression can be rearranged to give

$$\beta \cos \theta = \frac{K \lambda}{D} + 4\epsilon \sin \theta \quad (\text{Equation S8})$$

Plotting a graph with  $y = \beta \cos \theta$  and  $x = 4 \sin \theta$  allows us to determine the strain from the gradient and the crystallite size from the intercept.

The thickest sample (exposure time 3600 s, optical thickness 320 nm) has seven peaks which have strong enough intensity to find an accurate FWHM. We fitted the full XRD profile with a background and multiple Voigt functions to determine the angle and FWHM of each peak. The resulting Williamson-Hall plot is shown in Figure S6. The microstrain is determined directly from the gradient to be 0.16%. The intercept is equal to 0.0017 which, using the same values for  $K$  and  $\lambda$  as above, gives a crystallite height of 79 nm.

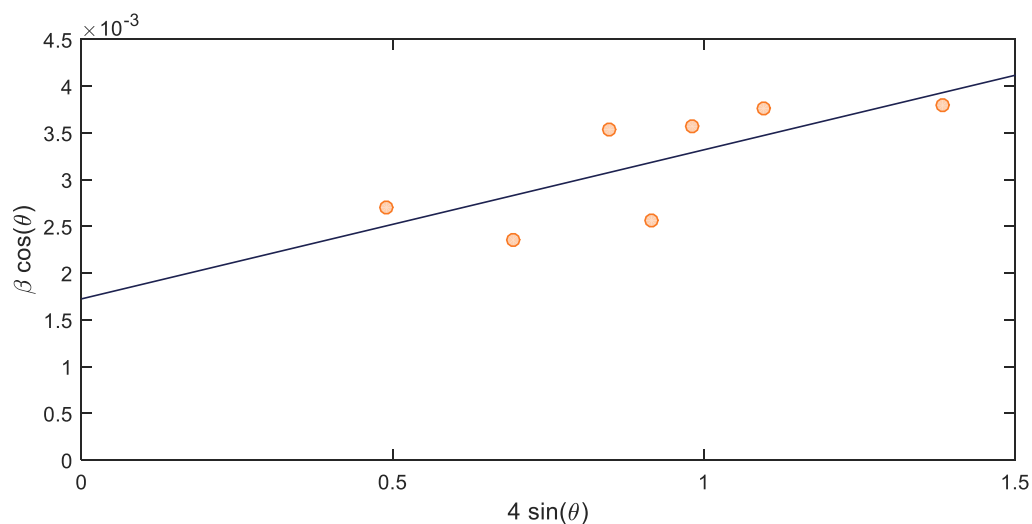


**Figure S6:** Williamson-Hall plot for the MAPbI<sub>3</sub> sample with 320 nm optical thickness.

## Correction of PL Spectra for Self-absorption

Since the PL spectrum and absorption spectrum overlap, some of the emitted PL will be reabsorbed by the material before escaping (self-absorption). According to Steiner et al.<sup>10</sup>, the escape probability from the front side of a film for a photon emitted at a depth  $x$  in the film is given by<sup>a</sup>

$$P(x, \lambda) = \frac{1}{2}(1 - R_f) \frac{e^{-\alpha x} + R_b e^{-\alpha(2L-x)}}{1 - R_f R_b e^{-2\alpha L}} \quad (\text{Equation S9})$$

where  $R_b$  is the probability of reflection from the back interface,  $R_f$  is the probability of reflection from the front interface,  $L=D/\cos\theta$ , and  $\theta$  is the angle of incidence of the emitted photon at the interface.

The angle  $\theta$  is determined via Snell's law by the collection angle given by the optics in our experiment. The reflection probabilities are determined by using the Fresnel equations, assuming no favored polarization. We use refractive indices of 2.5 for perovskite,<sup>3</sup> 1.0 for vacuum (front interface) and 1.5 for quartz (see Figure S8).<sup>3</sup>

The Fresnel equation giving the probability of reflection  $R$  for a mixture of parallel and plane polarised light is:

$$R = \frac{1}{2} \left( \frac{n_1 \cos(\theta_i) - n_2 \cos(\theta_t)}{n_1 \cos(\theta_i) + n_2 \cos(\theta_t)} \right)^2 + \frac{1}{2} \left( \frac{n_1 \cos(\theta_t) - n_2 \cos(\theta_i)}{n_1 \cos(\theta_t) + n_2 \cos(\theta_i)} \right)^2 \quad (\text{Equation S10})$$

For the front surface, the first medium is perovskite and the second medium is air with a transmission angle of  $5^\circ$  determined by the collection optics. The incident angle can be calculated from Snell's law:

$$\theta_i = \sin^{-1} \left( \frac{n_2}{n_1} \sin(\theta_t) \right) \quad (\text{Equation S11})$$

Thus  $n_1 = 2.5$ ,  $n_2 = 1$ ,  $\theta_t = 5^\circ$ ,  $\theta_i = 2^\circ$ ; giving a reflection probability of  $R_f = 18\%$ .

For the back surface, the first medium is perovskite and the second medium is quartz with an incident angle equal to that calculated above. The transmission angle can be calculated from Snell's law. Thus  $n_1 = 2.5$ ,  $n_2 = 1.5$ ,  $\theta_t = 3^\circ$ ,  $\theta_i = 2^\circ$ ; giving a reflection probability  $R_b = 6\%$ .

We can assume that photons originate equally from all depths of the film, since the initial charge carrier distribution becomes homogeneous by diffusion of carriers and by self-absorption quickly, compared with the PL lifetime of the sample.<sup>3</sup> To find the external intensity we also need to take into account the internal quantum efficiency and number of reabsorption events, however we are only

---

<sup>a</sup> Steiner's equation does not contain the factor  $1/2$ , but we believe this is in error. However this does not make a difference to the shape of the spectrum, which is what we are interested in.

interested in the shape of the spectrum. We can therefore integrate over all depths  $x$  to find the PL spectrum emitted from the film (the measured spectrum  $M(\theta)$ ) for a true PL spectrum  $I(\theta)$ :

$$M(\lambda) \propto I(\lambda) \frac{1}{L} \int_0^L P(x, \lambda) dx \quad (\text{Equation S12})$$

The real spectrum can then be calculated from the measured spectrum using

$$I(\lambda) \propto M(\lambda) \alpha L (1 - R_f R_b e^{-2\alpha L}) (1 - R_f)^{-1} (1 - e^{-\alpha L})^{-1} (1 + R_b e^{-\alpha L})^{-1} \quad (\text{Equation S13})$$

By substituting  $\alpha L = a/\cos\theta$ , we can use the measured absorbance without needing to know the thickness or absorption coefficient.

Figure S7 shows our measured and corrected PL spectra for the five samples where the substrate was fully covered. We assume that the effect of reabsorption is negligible for the thinnest two samples, since the island structure and the fact that these samples are less than 10 nm in thickness should enable light to escape easily and not be reabsorbed. In fact our calculations show that it is only the samples with optical thickness of 130 and 320 nm that show significant reabsorption.

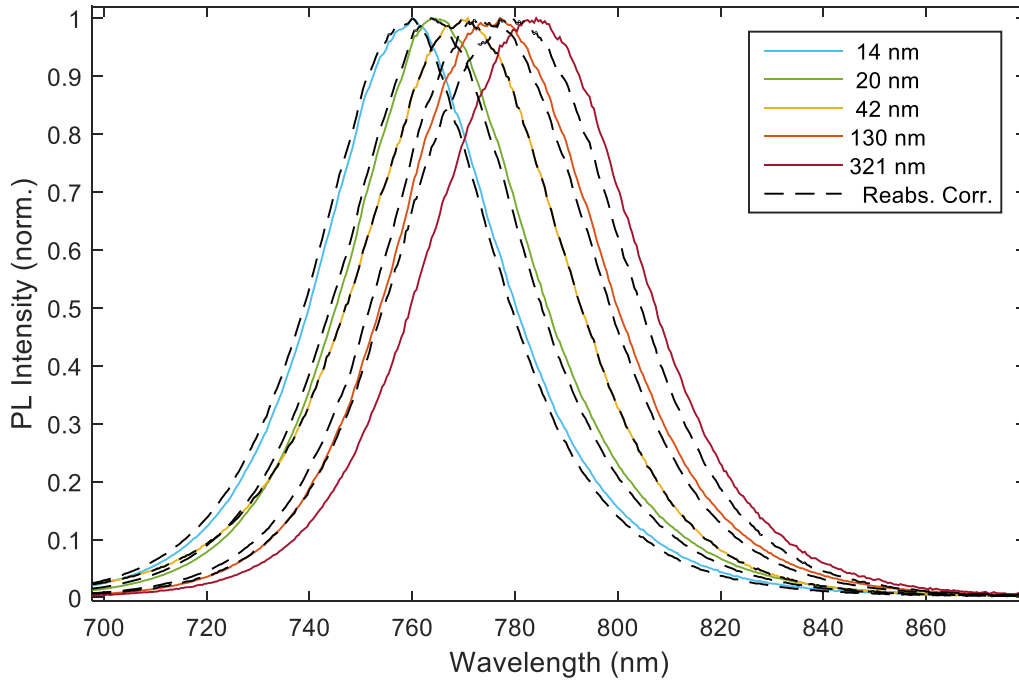


**Figure S7:** PL spectra for the MAPbI<sub>3</sub> samples with full coverage before (solid line) and after (dashed black line) correction for self-absorption. The legend shows the optical thickness of the perovskite.

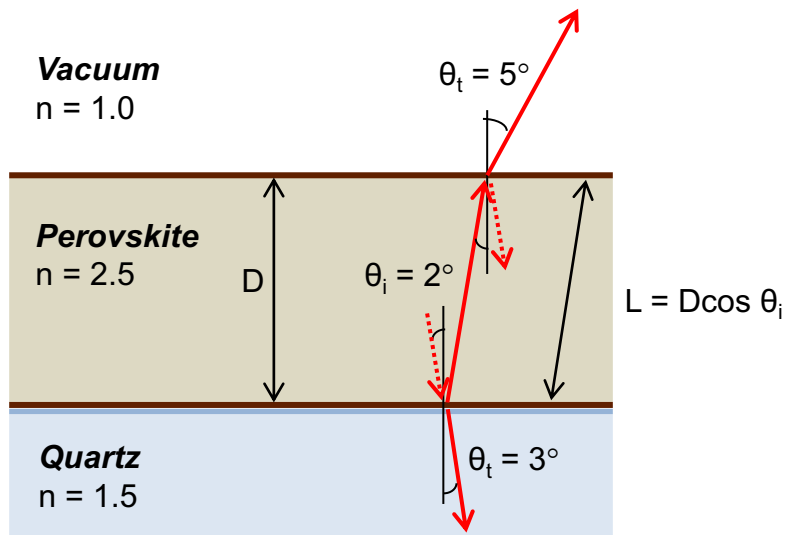


**Figure S8:** Schematic diagram showing relevant angles calculated in the reabsorption correction.

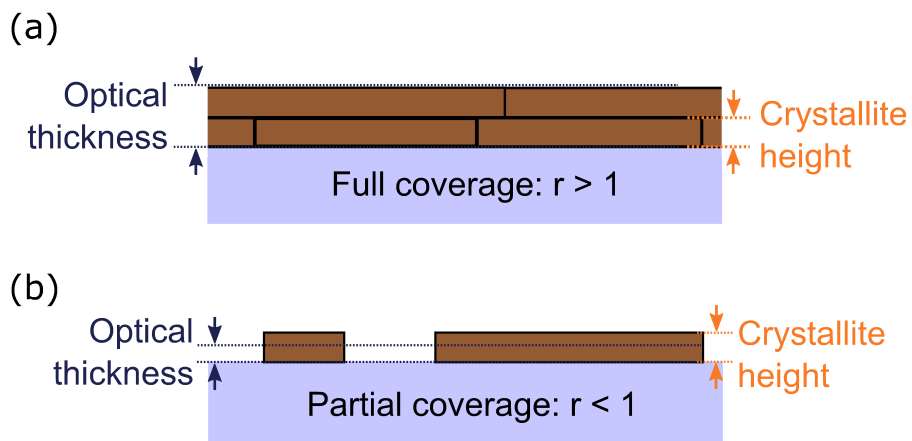


**Figure S9:** Schematic diagram showing the relevant thicknesses when the ratio  $r$  is (a) greater than 1 and (b) less than 1.

## References

- (1) Patel, J. B.; Wong-Leung, J.; Van Reenen, S.; Sakai, N.; Wang, J. T. W.; Parrott, E. S.; Liu, M.; Snaith, H. J.; Herz, L. M.; Johnston, M. B. Influence of Interface Morphology on Hysteresis in Vapor-Deposited Perovskite Solar Cells. *Adv. Electron. Mater.* **2017**, *3* (2), 1600470.
- (2) Liu, M.; Johnston, M. B.; Snaith, H. J. Efficient Planar Heterojunction Perovskite Solar Cells by Vapour Deposition. *Nature* **2013**, *501* (7467), 395–398.
- (3) Crothers, T. W.; Milot, R. L.; Patel, J. B.; Parrott, E. S.; Schlipf, J.; Müller-Buschbaum, P.; Johnston, M. B.; Herz, L. M. Photon Reabsorption Masks Intrinsic Bimolecular Charge-Carrier Recombination in CH<sub>3</sub>NH<sub>3</sub>PbI<sub>3</sub> Perovskite. *Nano Lett.* **2017**, *17* (9), 5782–5789.
- (4) Davies, C. L.; Filip, M. R.; Patel, J. B.; Crothers, T. W.; Verdi, C.; Wright, A. D.; Milot, R. L.; Giustino, F.; Johnston, M. B.; Herz, L. M. Bimolecular Recombination in Methylammonium Lead Triiodide Perovskite Is an Inverse Absorption Process. *Nat. Commun.* **2018**, *9* (1), 293.
- (5) Baikie, T.; Fang, Y.; Kadro, J. M.; Schreyer, M.; Wei, F.; Mhaisalkar, S. G.; Graetzel, M.; White, T. J. Synthesis and Crystal Chemistry of the Hybrid Perovskite (CH<sub>3</sub>NH<sub>3</sub>)PbI<sub>3</sub> for Solid-State Sensitised Solar Cell Applications. *J. Mater. Chem. A* **2013**, *1* (18), 5628.
- (6) Liu, Y.; Yang, Z.; Cui, D.; Ren, X.; Sun, J.; Liu, X.; Zhang, J.; Wei, Q.; Fan, H.; Yu, F.; et al. Two-Inch-Sized Perovskite CH<sub>3</sub>NH<sub>3</sub>PbX<sub>3</sub> (X = Cl, Br, I) Crystals: Growth and Characterization. *Adv. Mater.* **2015**, *27* (35), 5176–5183.
- (7) Dang, Y.; Liu, Y.; Sun, Y.; Yuan, D.; Liu, X.; Lu, W.; Liu, G.; Xia, H.; Tao, X. Bulk Crystal Growth of Hybrid Perovskite Material CH<sub>3</sub>NH<sub>3</sub>PbI<sub>3</sub>. *CrystEngComm* **2015**, *17* (3), 665–670.
- (8) Scherrer, P. Estimation of the Size and Internal Structure of Colloidal Particles by Means of Röntgen. *Göttinger Nachrichten Math. Phys.* **1918**, *2*, 98–100.
- (9) Langford, J. I.; Wilson, A. J. C. Scherrer after Sixty Years: A Survey and Some New Results in the Determination of Crystallite Size. *J. Appl. Cryst.* **1978**, *11*, 102–113.
- (10) Steiner, M. A.; Geisz, J. F.; García, I.; Friedman, D. J.; Duda, A.; Kurtz, S. R. Optical Enhancement of the Open-Circuit Voltage in High Quality GaAs Solar Cells. *J. Appl. Phys.* **2013**, *113* (12).